

Magnetic properties of a degenerate Anderson impurity

H. Q. Lin and J. E. Hirsch

Department of Physics, University of California, San Diego, La Jolla, California 92093

(Received 16 March 1987)

The properties of a doubly degenerate Anderson impurity in an electron gas are studied using a Monte Carlo simulation technique. The model is characterized by the intra-atomic Coulomb repulsion U , the exchange integral J , the hybridization width Δ , and the d electron energy level E_m . The effects of U and J on magnetic and orbital properties of the impurity are studied, and significant differences with predictions of Hartree-Fock theory are found. In particular, the condition for quenching of the orbital moment is found to be much less stringent than predicted by Hartree-Fock theory. The magnetic susceptibility is found to follow the universal Kondo behavior for both $J=0$ and $J\neq 0$. We also study the effect of crystal-field splitting on the Kondo temperatures, and find a surprisingly small effect for large crystal fields, in agreement with recent theoretical calculations. Our results provide an explanation for the quenching of the orbital angular momentum observed in transition metals and their alloys, and for the absence of magnetic order in certain dense Kondo systems.

I. INTRODUCTION

The magnetic properties of dilute alloys with transition-metal-atom impurities in a normal matrix have been studied for many years. The localized virtual-state picture presented by Friedel¹ have been used to explain numerous experimental results qualitatively and sometimes quantitatively. Based on Friedel's idea, Anderson² proposed a celebrated model, the Anderson model, for formulating the theory in a way that is more convenient for quantitative calculations. In the appendix of his paper,² Anderson generalized his model to one with double degeneracy. While the nondegenerate Anderson model has been studied extensively by several approaches and great success has been achieved, the model with degeneracy is less well understood. Moriya³ has studied a fivefold degenerate Anderson model for one and two impurities in the Hartree-Fock approximation scheme. Using the same approximation, Coqblin and Blandin⁴ have studied the doubly degenerate Anderson model extensively. The effects of magnetic anisotropy on the model have been studied by Yosida *et al.*⁵ with the same method. Like the nondegenerate Anderson model, a canonical transformation can also be used to relate the degenerate Anderson model to the Kondo model.⁶⁻⁸ The influence of the crystal field on the Kondo effect has been discussed by Cornut and Coqblin,⁹ by Nozieres and Blandin,¹⁰ and by Yamada *et al.*¹¹ Other approximate calculations have also been carried out like perturbation theory in the Coulomb repulsion energy,^{12,13} the Green's function approach of Lucas and Mattis,¹⁴ and a charge-transfer method by Oles and Chao.¹⁵ All these studies are based on some kind of approximation. Although they sometimes give correct answers in limiting cases, a nonperturbative study of the degenerate Anderson model is desirable especially for cases where various parameters of the model are of comparable size and many body correlations play an important role.

Computer simulations provide a way to study a model Hamiltonian nonperturbatively. For the magnetic impurity problem an efficient simulation method has been recently proposed.¹⁶ In this paper we will study the magnetic properties of the doubly degenerate Anderson impurity model by Monte Carlo simulations. Although in the transition metals the degeneracy is five instead of two, the cubic symmetric crystal field can split the d -electron energy into three and two degenerate levels (t_{2g} and e_g). The effects of degeneracy can be seen clearly from the study of the doubly degenerate Anderson model so it is of great theoretical interests.

In the following section we define all the parameters of the model Hamiltonian and discuss some previous results. In Sec. III we describe the simulation method we use to study the degenerate Anderson model and compare Monte Carlo results with exact diagonalization results to check their accuracy. We study the role of Hund's rule, the universal Kondo behavior, and the effects of crystalline potential in Sec. IV. Finally, we summarize and discuss our results in Sec. V. In the Appendix, we discuss the effect of a spin-flip term in the Hamiltonian.

II. MODEL HAMILTONIAN

The model we study has the form^{2,3}

$$H = H_c + H_d + H_{cd} \quad , \quad (1)$$

where

$$H_c = \sum_{\mathbf{k}, \sigma} \epsilon_{\mathbf{k}} n_{\mathbf{k}\sigma} \quad ,$$

$$H_d = \sum_{m, \sigma} E_m n_{m\sigma} + U \sum_{mm'} n_{m\uparrow} n_{m'\downarrow} \\ + \frac{1}{2}(U - J) \sum_{\substack{m \neq m' \\ \sigma}} n_{m\sigma} n_{m'\sigma} \quad ,$$

and

$$H_{cd} = \sum_{k,\sigma} \sum_m (V_{k,m} C_{k,\sigma}^\dagger C_{m\sigma} + V_{m,k} C_{m\sigma}^\dagger C_{k\sigma})$$

in Eq. (1). m and m' are the indices of the degenerate orbitals (1 or 2 here), E_m are the unperturbed d -level energies measured from the Fermi surface, U and J are the intra-atomic Coulomb repulsion energy and the exchange integral. For the transition metals the spin-orbit interaction is small compared to each part of the Hamiltonian and the crystalline potential so that we neglect it, and the impurity potential is assumed to be spherically symmetric. The angular momentum of a conduction electron is thus conserved and we can expand its wave function in spherical harmonics Y_l^m . The matrix element V_{km} of the hybridization in the usual case of $2l+1$ -fold degeneracy is given by

$$\begin{aligned} V_{km} &= \frac{1}{\sqrt{V}} \int e^{-i\mathbf{k}\cdot\mathbf{r}} V_{\text{imp}}(r) R_d(r) Y_l^m(\Omega_r) r^2 dr d\Omega \\ &= \frac{\sqrt{6\pi}}{kR} (-i)^l v_{kl} Y_l^m(\Omega_k), \end{aligned} \quad (2)$$

where $R_d(r)$ is the radial part of the d -electron wave function and v_{kl} is given by

$$v_{kl} = \sqrt{2/R} k \int j_l(kr) V_{\text{imp}}(r) R_d(r) r^2 dr.$$

For the doubly degenerate case we studied here, V_{km} is a linear combination of Y_l^m 's such that the average of $V_{km} V_{km'}$ over azimuthal angle is proportional to $\delta_{mm'}$. Let us define their phase factor such that

$$V_{km} = V_k R_m(\theta), \quad m = 1, 2$$

$$\delta_{mm'} = \langle R_m(\theta) R_{m'}(\theta) \rangle_\theta.$$

This Hamiltonian has been studied extensively via a set of Hartree-Fock self-consistent equations.⁴ Within the Hartree-Fock approximation, the Hamiltonian for an electron of spin σ can be written as

$$\begin{aligned} H_\sigma &= \sum_k \varepsilon_k n_{k\sigma} + \sum_m \tilde{E}_{m\sigma} n_{m\sigma} \\ &+ \sum_{km} (V_{km} C_{k\sigma}^\dagger C_{m\sigma} + V_{m,k} C_{m\sigma}^\dagger C_{k\sigma}), \end{aligned} \quad (3)$$

where

$$\tilde{E}_{m\sigma} = E_m + \sum_{m' \neq m} (U - J) n_{m'\sigma} + \sum_{m'} U n_{m' - \sigma}.$$

The diagonal elements of the Green's function are simply related to the density of states due to the mixture of the $|m, \sigma\rangle$ state with the continuum states:

$$\rho_{m\sigma}(E) = -\frac{1}{\pi} \text{Im} G_{mm'}^\sigma(E). \quad (4)$$

If we assume that the impurity potential is spherically symmetric then $G_{mm'}^\sigma$ can be written as

$$G_{mm'}^\sigma(E) = \frac{\delta_{mm'}}{E - \tilde{E}_{m\sigma} - \Gamma + i\Delta}, \quad (5)$$

with Γ and Δ independent of the orbital considered and the energy E .² Depending on the parameters U , J , Δ , and E_m , the ground state can have various kinds of ordering within the Hartree-Fock approximation.²⁻⁴ For instance, there will be no ordered ground state if $U + J < \pi\Delta$; whereas for $U - J < \pi\Delta < U + J$, the ground state will be spin ordered only, with orbital angular momentum quenched, and for $U - J > \pi\Delta$ the ground state will have both spin and orbital ordering. Although the Hartree-Fock approximation can give various analytical conclusions, it is a bad approximation for studying the magnetic properties of the transition metals. It neglects the correlations between electrons, and overestimates the tendency to magnetism. It is well known that the ground state for the nondegenerate Anderson model is a nonmagnetic singlet¹⁷ for any finite of the Coulomb repulsion U . For the degenerate case the ground will also be a nonmagnetic singlet rather than a triplet as we will see in the following.

Another way to study the Anderson impurity model is perturbation theory,¹⁸ in which one takes the Coulomb repulsion U or width of hybridization Δ as a perturbation. Taking the interaction part of the Hamiltonian as a perturbation in the degenerate impurity model, Shiba¹² and Yoshimori¹³ have derived a number of Ward identities satisfied by the various vertices, thus obtaining a relation between the specific heat and susceptibilities in the low-temperature limit. Resistivity was also discussed by them in the case of half-filled localized electrons. However, all these analyses were made at and near $T=0$ K, hence the results are restricted. No discussion was given on the change of the Kondo temperature T_K due to the degeneracy.

III. SIMULATION METHOD

To investigate the properties of a magnetic impurity with degenerate orbitals nonperturbatively we use a Monte Carlo technique, following a recently developed algorithm.¹⁶ We write the partition function as

$$\begin{aligned} Z &= \text{Tr} e^{-\beta H} = \text{Tr} \prod_{l=1}^L e^{-\Delta\tau(H_0(\tau_l) + H_I(\tau_l))} \\ &\approx \text{Tr} \prod_{l=1}^L e^{-\Delta\tau H_0(\tau_l)} e^{-\Delta\tau H_I(\tau_l)}, \end{aligned} \quad (6)$$

where $\beta = L\Delta\tau$, $H_0 = H - H_I$, and H_I is given by

$$\begin{aligned} H_I &= \frac{U}{2} (2n_{1\uparrow} n_{1\downarrow} - n_{1\uparrow} - n_{1\downarrow}) + \frac{U}{2} (2n_{2\uparrow} n_{2\downarrow} - n_{2\uparrow} - n_{2\downarrow}) + \frac{U}{2} (2n_{1\uparrow} n_{2\downarrow} - n_{1\uparrow} - n_{2\downarrow}) \\ &+ \frac{U}{2} (2n_{1\downarrow} n_{2\uparrow} - n_{1\downarrow} - n_{2\uparrow}) + \frac{(U-J)}{2} (2n_{1\uparrow} n_{2\uparrow} - n_{1\uparrow} - n_{2\uparrow}) + \frac{(U-J)}{2} (2n_{1\downarrow} n_{2\downarrow} - n_{1\downarrow} - n_{2\downarrow}). \end{aligned} \quad (7)$$

The six terms in the interaction part H_I all commute with each other and for each one of them we can decouple the interaction via a discrete Hubbard-Stratonovich transformation,¹⁹ say, for the $n_{1\uparrow}n_{1\downarrow}$ term

$$\begin{aligned} \exp[-\Delta\tau(U/2)(n_{1\uparrow}+n_{1\downarrow}-2n_{1\uparrow}n_{1\downarrow})] \\ = \frac{1}{2} \text{Tr}_\sigma \exp[\lambda(U)\sigma(n_{1\uparrow}-n_{1\downarrow})], \end{aligned}$$

where σ is an auxiliary Ising variable and the couplings $\lambda(U), \lambda(U-J)$ are given by the equation $\cosh(x) = \exp(\Delta\tau x/2)$. Taking the trace over fermion degrees of freedom the partition function can be written as

$$Z = \text{Tr}_{\{\sigma_{j,l}\}} \prod_{\mu=\uparrow\downarrow} \det O_\mu[\{\sigma_{j,l}\}], \quad j=1, \dots, 6 \quad (8)$$

where O_μ is an $(N+2)L \times (N+2)L$ matrix, with N the number of \mathbf{k} vectors for the conduction electrons. The matrix elements of O_μ are

$$[O_\mu]_{l,l} = I, \quad (9)$$

$$[O_\mu]_{l,l-1} = -e^{-\Delta\tau K} e^{V_l^\mu} (1 - 2\delta_{l,1}),$$

and $[O_\mu]_{l,l'} = 0$ otherwise. The matrix K corresponds to the noninteracting part of the Hamiltonian and V_l^μ is a diagonal matrix in space and time corresponding to the potential due to the auxiliary Ising fields which acts only at the two orbitals of the impurity site:

$$V_l^\mu = \Lambda(n_{1\mu}) |1\rangle\langle 1| + \Lambda(n_{2\mu}) |2\rangle\langle 2| \quad (10)$$

with

$$\Lambda(n_{1\uparrow}) = \lambda(U-J)\sigma_1 + \lambda(U)\sigma_3 + \lambda(U)\sigma_5,$$

$$\Lambda(n_{1\downarrow}) = \lambda(U-J)\sigma_2 - \lambda(U)\sigma_3 + \lambda(U)\sigma_6,$$

$$\Lambda(n_{2\uparrow}) = -\lambda(U-J)\sigma_1 + \lambda(U)\sigma_4 - \lambda(U)\sigma_6,$$

$$\Lambda(n_{2\downarrow}) = -\lambda(U-J)\sigma_2 - \lambda(U)\sigma_4 - \lambda(U)\sigma_5.$$

The Green's function matrix $G_\mu = O_\mu^{-1}$ satisfies the Dyson equation:

$$G'_\mu = G_\mu + (G_\mu - I)(e^{V' - V} - I)G'_\mu. \quad (11)$$

Our Monte Carlo strategy is simple: first we set both U and J equal to zero and then calculate the noninteracting Green's function, next we put in arbitrary initial Ising fields and obtain the d -electron Green's function by inverting a $2L \times 2L$ matrix. The Metropolis algorithm is used to determine whether an Ising spin $\sigma_j(l)$ is flipped and all the time components of the d -electron Green's functions $G_\mu(m, m'; l, l')$ are updated through the Dyson equation. Along the Monte Carlo's updating, we measure various interesting quantities such as the magnetic susceptibility χ_m , and study the properties of the system nonperturbatively.

For the algorithm we use, the error only comes from the breakup used in Eq. (6), which is proportional to $\Delta\tau^2$. We can reduce the systematic error by reducing $\Delta\tau$, i.e., increasing the number of time slices L , but the computer time increases as L^3 and the smaller $\Delta\tau$ is the more Monte Carlo sweeps are needed to reach equilibri-

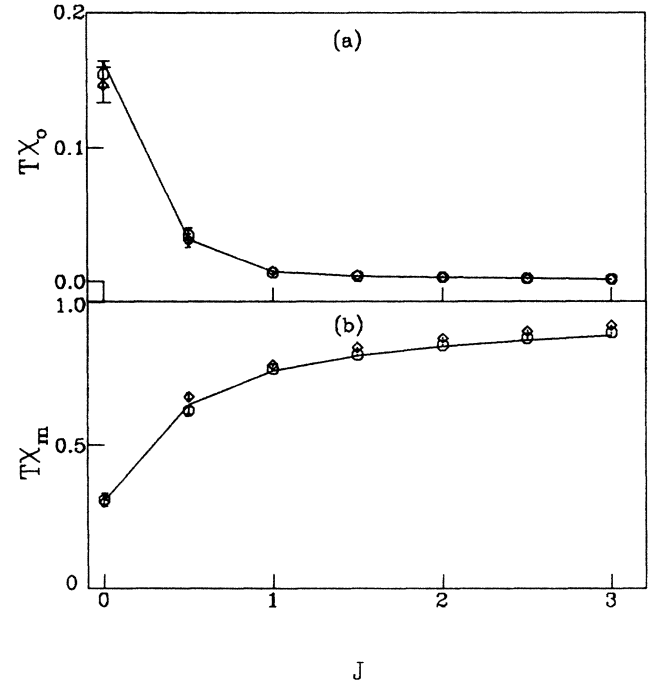


FIG. 1. Comparison of Monte Carlo (symbols) and exact diagonalization results (solid line) for (a) $T \times$ orbital susceptibility χ_0 , and (b) $T \times$ spin susceptibility χ_m as a function of J for a single degenerate Anderson impurity with a two-site conduction electron lattice. $U=4$, $T=0.125$; and $\Delta\tau=0.25$ (octagon), $\Delta\tau=0.50$ (diamond).

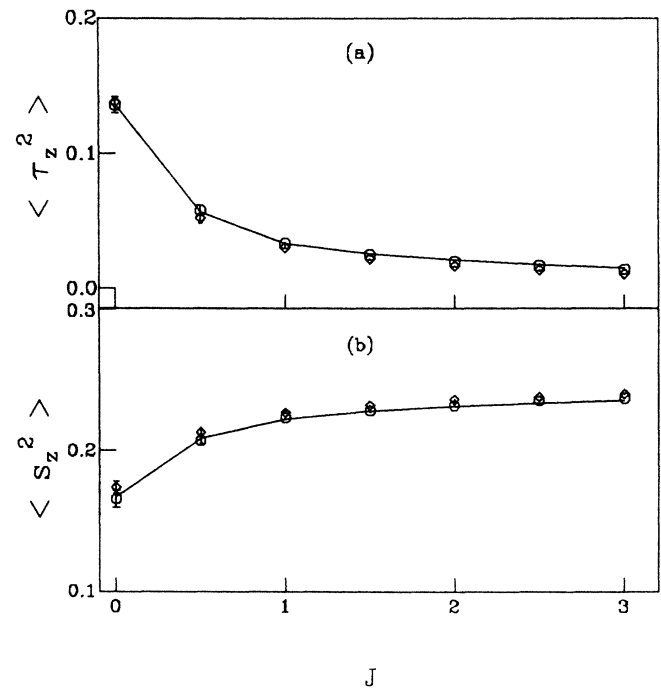


FIG. 2. Comparison of Monte Carlo (symbols) and exact diagonalization results (solid line) for (a) $\langle \tau_z^2 \rangle$, and (b) $\langle S_z^2 \rangle$ as a function of J for a single degenerate Anderson impurity with a two-site conduction electron lattice. $U=4$, $T=0.125$; and $\Delta\tau=0.25$ (octagon), $\Delta\tau=0.50$ (diamond).

um. To test our program as well as to choose an appropriate value of $\Delta\tau$, in Figs. 1 and 2 we compare our Monte Carlo results (symbols) of $T\chi_m$, $T\chi_0$, $\langle S_z^2 \rangle$, $\langle \tau_z^2 \rangle$, to be defined below, as function of J for $U=4.0$, $T=0.125$, with the results obtained from diagonalizing the Hamiltonian exactly (solid lines) for a two-site conduction-electron system. As we can see, the program works very well and for values of $\Delta\tau=0.25$, or even $\Delta\tau=0.50$, the systematic error is smaller than the statistical error. Most results presented in this paper were obtained on the Cray X-MP at the San Diego Supercomputer Center. The code is very easy to vectorize and the CPU time for a typical run of 10000 Monte Carlo

sweeps with $L=16$ time slices and 50% acceptance is about 11 min.

IV. RESULTS FOR THE DOUBLY DEGENERATE ANDERSON IMPURITY

In this section we present our Monte Carlo simulation results for the doubly degenerate Anderson impurity model. We will discuss the formation of the local moment, and the effect of crystal-field splitting. First we define the quantities to be studied. We define the magnetic susceptibility χ_m and the orbital susceptibility χ_0 by

$$\chi_m = \int_0^\beta d\tau \langle [n_{1\uparrow}(\tau) + n_{2\uparrow}(\tau) - n_{1\downarrow}(\tau) - n_{2\downarrow}(\tau)][n_{1\uparrow}(0) + n_{2\uparrow}(0) - n_{1\downarrow}(0) - n_{2\downarrow}(0)] \rangle,$$

$$\chi_0 = \int_0^\beta d\tau \langle [n_{1\uparrow}(\tau) + n_{1\downarrow}(\tau) - n_{2\uparrow}(\tau) - n_{2\downarrow}(\tau)][n_{1\uparrow}(0) + n_{1\downarrow}(0) - n_{2\uparrow}(0) - n_{2\downarrow}(0)] \rangle.$$

The spin-spin and orbital-orbital correlation functions are defined by

$$\langle S_z^2 \rangle = \frac{1}{2} \sum_{m=1}^2 \frac{1}{4} \langle (n_{m\uparrow} - n_{m\downarrow})^2 \rangle,$$

$$\langle S_{1z} S_{2z} \rangle = \frac{1}{4} \langle (n_{1\uparrow} - n_{1\downarrow})(n_{2\uparrow} - n_{2\downarrow}) \rangle,$$

$$\langle \tau_z^2 \rangle = \frac{1}{2} \sum_{\sigma} \frac{1}{4} \langle (n_{1\sigma} - n_{2\sigma})^2 \rangle,$$

$$\langle \tau_{1z} \tau_{2z} \rangle = \frac{1}{4} \langle (n_{1\uparrow} - n_{2\uparrow})(n_{1\downarrow} - n_{2\downarrow}) \rangle.$$

The magnetic local moment $\langle S_z^2 \rangle$ defined above is for the single orbital and the total moment is just twice of $\langle S_z^2 \rangle + \langle S_{1z} S_{2z} \rangle$. Similarly, the total orbital moment is $2(\langle \tau_z^2 \rangle + \langle \tau_{1z} \tau_{2z} \rangle)$. For the Hamiltonian, Eq. (1), there exist certain kinds of symmetries. For the case of no crystalline field, $E_1=E_2$, it can be shown that $\langle \tau_{1z} \tau_{2z} \rangle = 0$ identically by a canonical transformation: $R_1(\theta)C_{1\uparrow} \rightarrow R_2(\theta)C_{2\uparrow}$, $R_2(\theta)C_{2\uparrow} \rightarrow R_1(\theta)C_{1\uparrow}$; $C_{1\downarrow} \rightarrow C_{1\downarrow}$, $C_{2\downarrow} \rightarrow C_{2\downarrow}$. If the exchange integral $J=0$, the system is rotationally invariant in spin space and it is easy to show that $\chi_m = \chi_0$, $\langle S_z^2 \rangle = \langle \tau_z^2 \rangle$, and $\langle S_{1z} S_{2z} \rangle = \langle \tau_{1z} \tau_{2z} \rangle = 0$ by a canonical transformation: $R_1(\theta)C_{1\downarrow} \rightarrow R_2(\theta)C_{2\uparrow}$, $R_2(\theta)C_{2\uparrow} \rightarrow R_1(\theta)C_{1\downarrow}$; $C_{1\uparrow} \rightarrow C_{1\uparrow}$, $C_{2\downarrow} \rightarrow C_{2\downarrow}$.

The system we are studying has a quite large parameter space. Throughout this paper we chose a flat density of states with an infinite bandwidth and we set the widths of the hybridization to be the same for both orbitals $\Delta = \pi V^2 \rho(E_F) = 0.5$, where $\rho(E_F)$ is the density of state at the Fermi level. The properties of the system depend on the Coulomb repulsion energy U , the exchange integral J , the d -level energy E_1 and E_2 , and the temperature T . The Green's functions for U and J equal to zero are

$$G_{mm'}(l, l') = T \sum_n e^{i\omega_n \Delta\tau(l-l')} G_{mm'}(i\omega_n), \quad (12)$$

$$G_{mm'}(i\omega_n) = -\delta_{mm'} \left[i\omega_n - E_m - \sum_k \frac{|V_{km}|^2}{i\omega_n - e_k} \right]^{-1},$$

where $\omega_n = (2n+1)\pi/\beta$. In the following subsections we discuss the effect of U and J on spin and orbital magnetism, the universal Kondo behavior, and finally the effect of crystal-field splitting.

A. Spin and orbital magnetism

We consider the half-filled band case, i.e., $E_1 = E_2 = -(3U - J)/2$ so that $\langle n_{im} \rangle = 1$, independent of temperature because of particle-hole symmetry. Results for $U=4$ as a function of J are shown in Fig. 3 at temperature $T=0.125$. We see that the magnetic susceptibility χ_m and the magnetic local moment $\langle S_z^2 \rangle$ and spin-spin correlation $\langle S_{1z} S_{2z} \rangle$ increases as J increases while the orbital susceptibility χ_0 and the orbital-local moment $\langle \tau_z^2 \rangle$ behave in an opposite way, in accordance with Hund's rule and in qualitative agreement with Hartree-Fock solutions. In Figs. 4 and 5 we show results as a function of U for $J=0$, and 0.5 at the same temperature. They do not depend on U as strongly as for the nondegenerate case. As a matter of fact, when $J=0$, the magnetic local moment $\langle S_z^2 \rangle$ varies from its noninteracting value 0.125 to $\frac{1}{6}$ at the atomic limit, $U \rightarrow \infty$, whereas it goes to 0.25 at the atomic limit in the nondegenerate case. For $J=0$, both the orbital and magnetic moments are very slowly increasing functions of U , for finite value of J ($=0.5$ in Fig. 5), however, the effect of U is quite different: it enhances the magnetic moment much more strongly, while it suppresses the orbital moment; in contrast, within the Hartree-Fock ap-

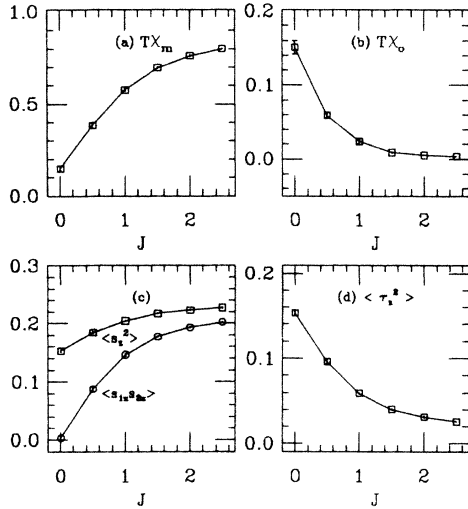


FIG. 3. (a) $T \times$ spin susceptibility χ_m , (b) $T \times$ orbital susceptibility χ_o , (c) magnetic local moment $\langle S_z^2 \rangle$ and spin-spin correlation $\langle S_{1z} S_{2z} \rangle$, and (d) orbital local moment $\langle \tau_z^2 \rangle$ as a function of J for $T=0.125$, $U=4$; $\Delta=0.5$, $\Delta\tau=0.25$.

proximation the effect of U in the presence of J is predicted to be qualitatively the same as for $J=0$, in particular, the orbital moment is always enhanced by U .

B. Universal Kondo behavior

For a nondegenerate Anderson impurity at sufficiently low temperatures, the Kondo effect leads to the spin of

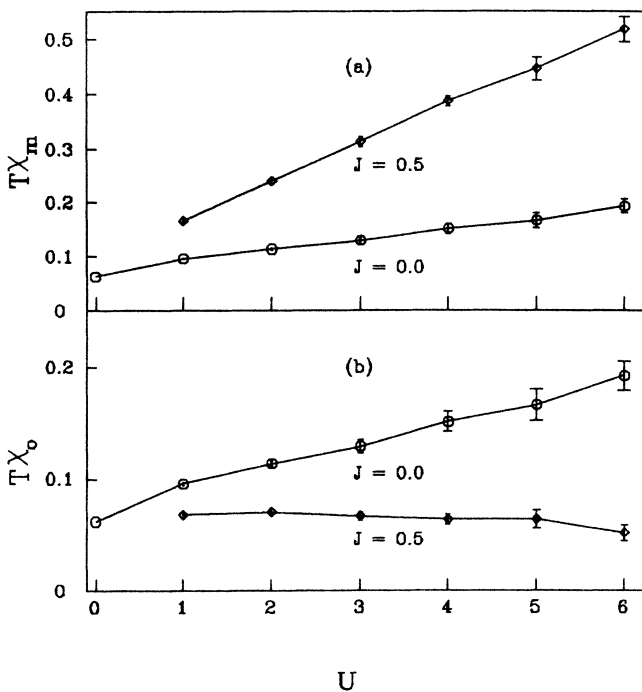


FIG. 4. (a) $T \times$ spin susceptibility χ_m , and (b) $T \times$ orbital susceptibility χ_o as function of U for $T=0.125$, $J=0.0, 0.5$; $\Delta=0.5$, $\Delta\tau=0.25$.

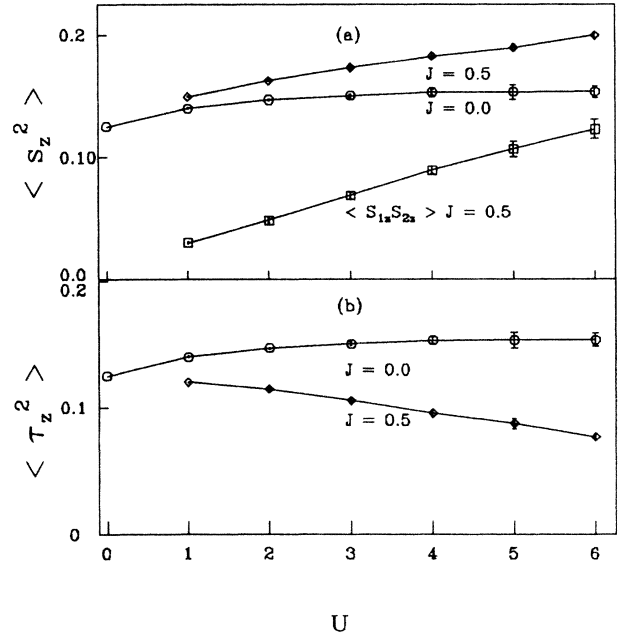


FIG. 5. (a) Magnetic local moment $\langle S_z^2 \rangle$ and spin-spin correlation $\langle S_{1z} S_{2z} \rangle$, and (b) orbital local moment $\langle \tau_z^2 \rangle$ as a function of U for $T=0.125$, $J=0.0, 0.5$; $\Delta=0.5$, $\Delta\tau=0.25$.

the localized moment being totally compensated by the spins of a cloud of conduction electrons. This is expected to be also true for the degenerate Anderson impurity. The conduction electrons will keep the same orbital angular momentum before and after being scattered by the impurity. Thus each spin of the localized moment in its own orbital will be totally screened by the conduction electrons with the same orbital angular momentum. Several authors have used the Schrieffer-Wolff (SW) transformation to relate the degenerate Anderson model to the Kondo model.⁶⁻¹⁰ Although they differ from each other somewhat, the results are essentially the same. However, the SW transformation is a second-order perturbation in which the atomic part of the Hamiltonian is much larger than the hybridization part so the results do not relate to the degenerate Anderson model directly. With Bethe ansatz one can get a solution for the degenerate Anderson model with an infinite U (Ref. 20) but it is hard to get the correlations function even in this infinite U limit. In this section we present our simulation results for the magnetic susceptibility and local moments.

We find, as one expects, that the system develops a localized moment and the Kondo effect leads to the compensation of the moment as the temperature is lowered. For the nondegenerate Anderson impurity it is shown that the magnetic susceptibility χ_m follows a universal curve²¹ for temperature $T < \Delta$. For the doubly degenerate Anderson impurity we find that the magnetic susceptibility χ_m also follows the universal curve. In Fig. 6 we show the results of $T\chi_m$ versus $\ln T$ for the cases of $U=1, 2, 3, 4$ and $J=0$. The solid lines there are the universal curve with the Kondo temperatures indicated

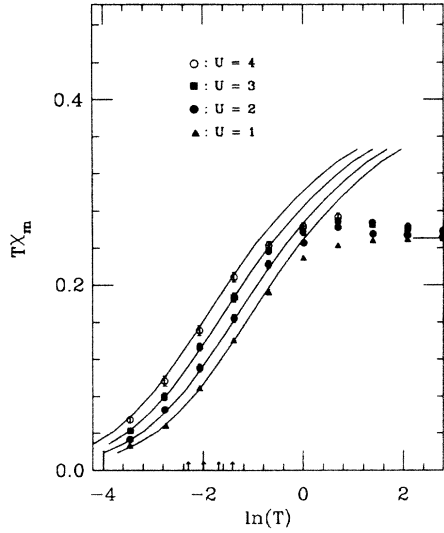


FIG. 6. $T \times$ spin susceptibility χ_m for $U=1, 2, 3, 4$, and $J=0$; the solid lines are the universal Kondo curves for the four values of T_K given in the text and indicated by arrows. $\Delta=0.5$, $\Delta\tau=0.25$.

by the arrows in the figure and given by the following formula:

$$T_K = D_0 e^{-(\pi U/8\Delta M)}, \quad (13)$$

where M is degeneracy number, which is 2 in our case. The Kondo temperatures for the cases studied are $T_K=0.2503$, $U=1$; $T_K=0.1897$, $U=2$; $T_K=0.1413$, $U=3$; and $T_K=0.1039$, $U=4$. We see that the Kondo temperatures for the degenerate case are much higher than for the nondegenerate case. Our estimated Kondo temperatures fit Eq. (13) within an uncertainty $|\Delta T_K/T_K| < 5\%$. The exponential dependence, i.e., the factor $1/M$ in Eq. (13) can be obtained via a SW transformation. The prefactor D_0 used in Eq. (13) is assumed to be the same as in the nondegenerate case. We don't have an analytical solution here to justify this assumption. The correction to the prefactor, if this assumption is wrong, will be very small according to our numerical calculation.

When $J \neq 0$, the system is not rotationally invariant in spin space and some equalities like $\chi_m = \chi_0$ showed before do not hold. The magnetic susceptibility χ_m , however, still follows the universal curve as shown in Fig. 7, where the parameters and the corresponding Kondo temperatures are (a) $U=1$, $T_K=0.157$; $U=2$, $T_K=0.0973$ for $J=0.25$, and (b) $U=1$, $T_K=0.0907$; $U=2$, $T_K=0.0408$ for $J=0.05$. These Kondo temperatures are much lower than that of the $J=0$ case because of the Hund's coupling. In Fig. 8 we show the temperature dependence of the orbital susceptibility χ_0 for $J=0.25$, $U=1$ and 2. It depends on U weakly, is smaller than the magnetic susceptibility χ_m and decreases somewhat more slowly with temperature.

We also show results for the magnetic local moments $\langle S_z^2 \rangle$ and the spin-spin correlation $\langle S_{1z} S_{2z} \rangle$ in Figs. 9

and 10 for the same parameters used for the susceptibility. The local moment forms at temperature $T \approx \Delta$, and slightly decreases at lower temperatures. According to the Hartree-Fock solutions,²⁻⁴ the ground state will be magnetic if $U + J/\pi\Delta \geq 1$. Although results based on the Hartree-Fock approximation are incorrect in most cases, this criterion seems approximately true if used for judging the appearance of the susceptibility peak at intermediate temperatures. We can see from Figs. 6 and 7 that $T\chi_m$ increases first as the temperature is lowered, indicating that the system develops a localized magnetic moment, for the cases $J=0$, $U=2, 3, 4$; $J=0.25$, $U=2$; and $J=0.5$, $U=1, 2$, and then drops to zero as the temperature goes to zero due to the Kondo compensation,

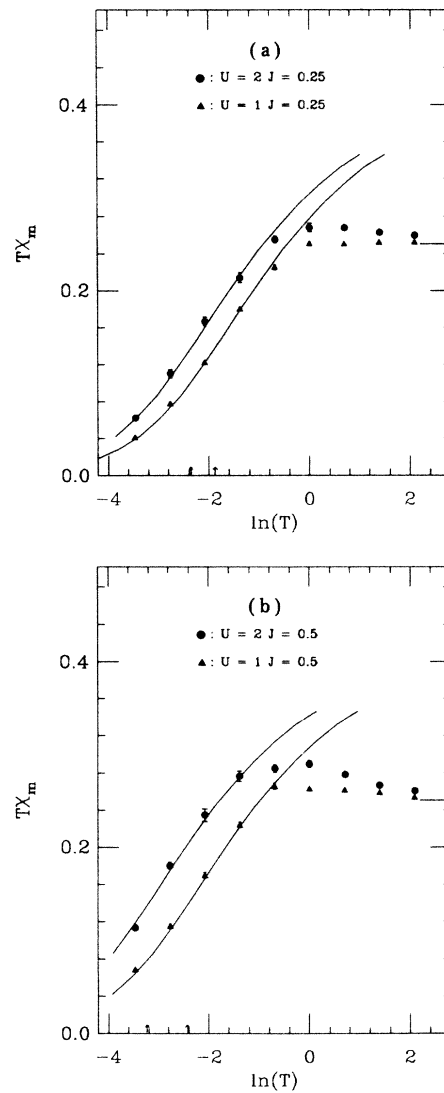


FIG. 7. (a) $T \times$ spin susceptibility χ_m for $U=1, 2$, and $J=0.25$; the solid lines are the universal Kondo curves for the two values of T_K given in the text and indicated by arrows. $\Delta=0.5$, $\Delta\tau=0.25$. (b) $T \times$ spin susceptibility χ_m for $U=1, 2$, and $J=0.5$; the solid lines are the universal Kondo curves for the two values of T_K given in the text and indicated by arrows. $\Delta=0.5$, $\Delta\tau=0.25$.

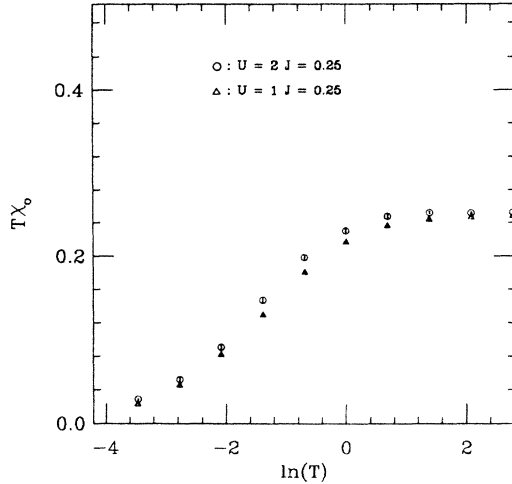


FIG. 8. $T \times$ orbital susceptibility χ_0 for $U=1, 2$, and $J=0.25$; $\Delta=0.5$, $\Delta\tau=0.25$.

while for the cases $U=1, J=0$ and 0.25 , $T\chi_m$ decreases to zero monotonically, showing that the system is compensated before it develops the local moment. Note that the number 1 used in the above criterion should not be taken too seriously. The results for the orbital local moment $\langle \tau_z^2 \rangle$ are shown in Fig. 11. Unlike the magnetic case, the orbital local moment increases somewhat as the temperature approaches zero. Our results agree with the Hartree-Fock prediction that the orbital local moment is an increasing function of $U-J$, they show that J suppresses the orbital moment rapidly, while U can either enhance or suppress it depending on the value of J . It is obvious that the disagreement between our results and the Hartree-Fock solutions does not come from symmetry breaking because the Hartree-Fock approximation starts from breaking the symmetry, even the up-down symmetry in the z direction. In fact, as mentioned by Coqblin and Blandin,⁴ the set of Hartree-Fock self-consistent equations does not change at all when including the spin-flip term for preserving the rotational symmetry in spin space.

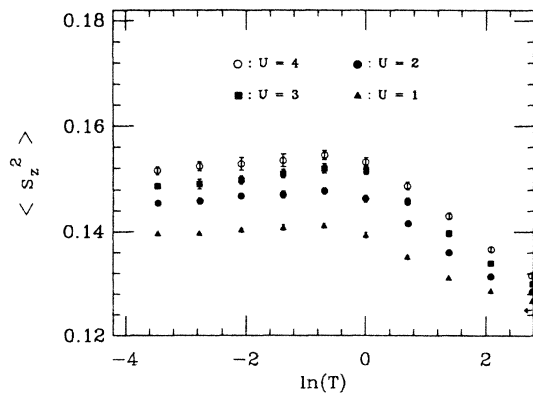


FIG. 9. Magnetic and orbital local moment $\langle S_z^2 \rangle = \langle \tau_z^2 \rangle$ for $U=1, 2, 3, 4$, and $J=0$; the arrow indicates the high-temperature limit. $\Delta=0.5$, $\Delta\tau=0.25$.

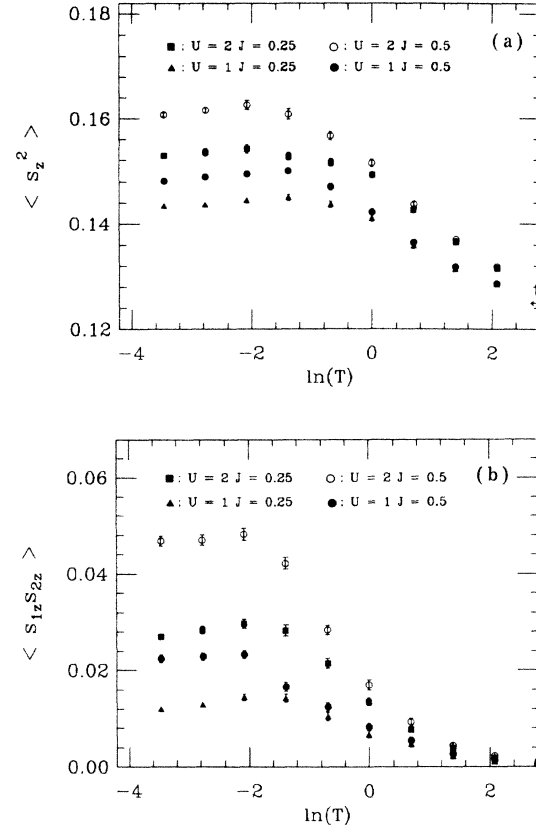


FIG. 10. (a) Magnetic local moment $\langle S_z^2 \rangle$ for $U=1, 2$, and $J=0.25, 0.5$; the arrow indicates the high-temperature limit. $\Delta=0.5$, $\Delta\tau=0.25$. (b) Spin-spin correlation $\langle S_{1z}S_{2z} \rangle$ for $U=1, 2$, and $J=0.25, 0.5$; the high-temperature limit is zero. $\Delta=0.5$, $\Delta\tau=0.25$.

C. Crystal-field splitting

One important feature about transition-metal ions is that the unpaired electrons lie in the outermost shell of the ion. Therefore they are easily influenced by the external charge distribution of their neighboring ions so

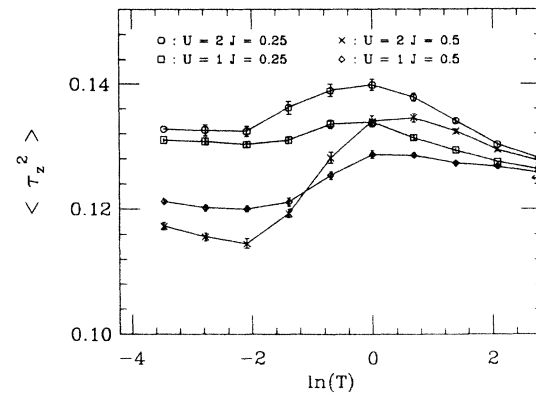


FIG. 11. Orbital-local moment $\langle \tau_z^2 \rangle$ for $U=1, 2$, and $J=0.25, 0.5$; the arrow indicates the high-temperature limit. $\Delta=0.5$, $\Delta\tau=0.25$.

that the crystal-field term should be included in the Hamiltonian even though it is quite smaller than the atomic part of the Hamiltonian. We can simply lump the crystal-field splitting effect into the unperturbed d -electron energy level E_m such that $E_1 \neq E_2$, where the only changes made are the representations of the wave functions for impurity and conduction electrons if we consider a cubic symmetry case.⁹ When taking the crystalline potential into account the system might be quite complicated:¹⁰ the Fermi surface of the host may become anisotropic, the widths of the hybridization will be different in different orbitals and depend on energy, etc. We will neglect these effects assuming they are not very important, especially in the low-temperature regime. The noninteracting Green's functions, i.e., the inputs in the Monte Carlo simulations are obtained from the same expression as before [Eq. (12)]. The crystal-field (CF) splitting effect are measured by $\Delta E_d = E_2 - E_1$. In Fig. 12 we show the results of $T\chi_m$ versus $\ln T$ for the case of $U=2, J=0$, and $\Delta E_d=0, 1$, and 2. The solid line is the universal Kondo curve with $T_K=0.333 \pm 0.017$ corresponding to no CF case $E_1 = E_2 = -U/2$. (For the case of $U=1, 3$, and 4, we found the same results, i.e., the magnetic susceptibility χ_m following the universal Kondo curve.) As we can see from the figure, above the Kondo temperature the magnetic susceptibility is suppressed as the crystal field increases. However, as the temperature drops below the Kondo temperature they become more or less identical. As pointed out by Cornut and Coqblin,⁹ there exists a $\ln T$ high-temperature behavior, a $\ln T$ low-temperature behavior, and an intermediate $\ln T$ behavior in the presence of the crystalline field. So they do not follow the universal Kondo curve for higher temperature as in the case without the crystal field. Another point worth mentioning is the importance of the two d -level mixing. One at first might think that as one of the d levels move far

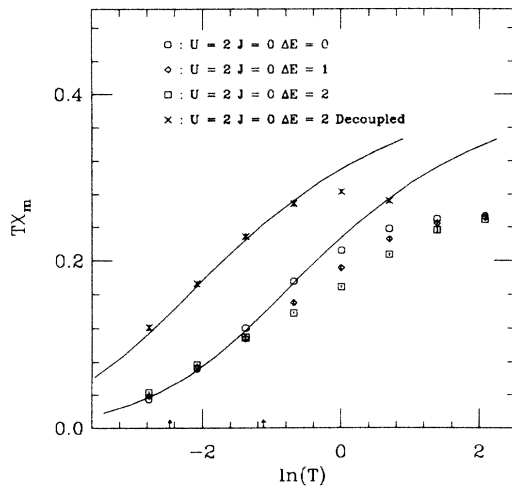


FIG. 12. $T \times$ spin susceptibility χ_m for $U=2, J=0$, $\Delta E_d=0.0$ (octagon), 1.0 (diamond), 2.0 (square), and decoupled two degenerate levels (cross). The solid line is the universal Kondo curve for the case of $\Delta E_d=0$ with $T_K=0.333 \pm 0.017$. $\Delta=0.5, \Delta\tau=0.25$.

apart from the other one the result will be close to that of the nondegenerate impurity. This is incorrect as shown in Fig. 12. However, if we decouple the two d levels by setting U and J equal to zero for electrons in different orbitals in the Hamiltonian then the results become identical to the nondegenerate case as one expects. We also show this result in Fig. 12 (crosses), with Kondo temperature $T_K=0.0865$. Our results show that the participation of the other level, though it is small ($\langle n_2 \rangle = 0.14$ for $\Delta E_d = U$), is important for increasing the Kondo temperature, in agreement with the result obtained by Yamada *et al.*¹¹ using scaling theory for the dense Kondo system.

V. CONCLUSION AND DISCUSSION

We have studied magnetic properties of a doubly degenerate Anderson impurity model using a Monte Carlo simulation technique. Our results for the model are essentially exact, as demonstrated by the agreement of Monte Carlo and exact diagonalization results for a particular case (Sec. III).

Just as in the nondegenerate case, the model displays no sharp phase transition as a function of the parameters, as one expects. Still, it is of interest to compare its properties qualitatively with the predictions of Hartree-Fock (HF) theory, because previous studies are mostly based on it. For the properties related to spin magnetism (spin magnetic moment and susceptibility) Hartree-Fock gives roughly qualitatively correct answers: they are enhanced by both U and J . However, contrary to HF predictions it is not the condition $(U+J)/\pi\Delta$ that is relevant, since the effect of J is markedly more pronounced than that of U ; in neglecting the effect of correlations between electrons of opposite spin, HF overestimates the effect of U . The discrepancy becomes more pronounced for the orbital properties (orbital magnetic moment and susceptibility). Here, HF predicts that the relevant parameter is $(U-J)/\pi\Delta$, and orbital magnetism should be zero or monotonically increasing with $U-J$. In contrast, we found that the orbital moment and susceptibility are slightly enhanced by U for $J=0$ but suppressed by U for $J=0.5$ as shown in Figs. 4(b) and 5(b). Thus our results have shown that to have the orbital angular momentum quenched the condition $U-J < \pi\Delta$ is not required. The fact that in transition metals and their alloys the orbital angular momentum is found to be always quenched, even in cases where U is expected to be substantially larger than J , is qualitatively explained by our observations, while one needs considerable fine tuning of the parameters within the Hartree-Fock approximation.³

Our results also showed that the Kondo compensation occurs similarly in the orbitally degenerate case as in the nondegenerate case. For $J=0$, the magnetic susceptibility χ_m is the same as the orbital susceptibility χ_0 and they follow the universal Kondo curve with the Kondo temperature given by Eq. (13). For $J \neq 0$, the magnetic susceptibility χ_m was again found to follow the universal Kondo curve, with a substantially reduced Kondo temperature. Finally, we have studied the effect of crystal-

line potential on the Kondo temperature. In agreement with recent calculations, our results showed that the effect of a crystal field is much smaller than one might have expected, in that the Kondo temperature T_K is not affected much by the presence of a crystal field ΔE_d even for $\Delta E_d \gg T_K$. As discussed by previous authors,⁹⁻¹¹ this provides an explanation for the absence of magnetic ordering in dense cerium compounds.

As emphasized by Coqblin and Blandin,⁴ the Hartree-Fock approximation suffers from two defects: it neglects correlations of electrons of opposite spin, and it breaks the spin-rotational invariance. In the present calculations we have remedied the first defect, but only partially the second; while our Hamiltonian does not break the up-down spin symmetry, it does break the full rotational symmetry in spin space for $J \neq 0$. This can be corrected, as described by Caroli *et al.*,²² Dworin and Narath,²³ and Parmenter.²⁴ The additional term to Eq. (1) is

$$-\frac{1}{2}J_{\pm} \sum_{m \neq m'} C_{m\sigma}^{\dagger} C_{m-\sigma} C_{m'-\sigma}^{\dagger} C_{m'\sigma} + \frac{1}{2}J_{\pm} \sum_{m\sigma} n_{m\sigma} n_{m-\sigma}. \quad (14)$$

It appears to be possible to include this term in a Monte Carlo calculation, although it becomes considerably more complicated. In the Appendix we discuss some exact results including this spin-flip term in the Hamiltonian.

An important question in the theory of magnetism is whether band degeneracy is essential for metallic ferromagnetism in transition metals and their alloys. Recently we have studied the nature of the magnetic interaction between two nondegenerate magnetic impurities in a metal that are coupled through a direct transfer integral.²⁵ We found that the impurities never display ferromagnetic correlations, in contradiction with previous results based on the Hartree-Fock approximation.²⁶ Ferromagnetic correlations may appear when there are degenerate orbitals, and we are currently investigating this question²⁷ by studying a pair of degenerate Anderson impurities.

APPENDIX

As we discussed in the conclusion, to have a rotationally invariant Hamiltonian the spin-flip term Eq. (14) should be included. To obtain a qualitative idea of the effect of this term we have studied the degenerate impurity with a two-site conduction electron system by exact

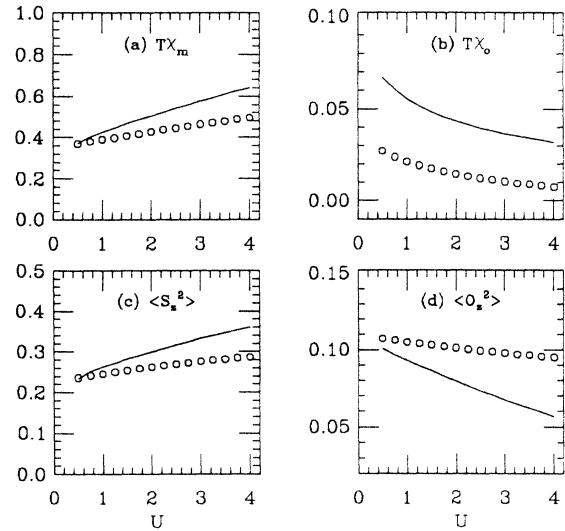


FIG. 13. (a) $T \times$ spin susceptibility χ_m , (b) $T \times$ orbital susceptibility χ_o , (c) total magnetic moment $\langle S_x^2 \rangle$, and (d) total orbital moment $\langle \tau_x^2 \rangle$ as function of U for $J=0.5$ and $J_{\pm}=0$ (solid lines), $J=0.5$ and $J_{\pm}=J$ (octagon); $T=0.125$, $\Delta=0.5$, $\Delta\tau=0.25$.

diagonalization with and without the spin-flip term. Figure 13 shows results for various quantities at $\beta=8$ for $J=0.5$, $J_{\pm}=0$ and $J_{\pm}=0.5$. The dependence on U does not change qualitatively when the spin-flip term is included: the spin-spin correlation and susceptibility are enhanced by U , while the orbital-orbital correlation and susceptibility are suppressed. The effect of J_{\pm} is to suppress the spin and orbital susceptibilities with respect to the case $J_{\pm}=0$. The spin-spin correlation is suppressed while the orbital-orbital correlation is enhanced. We expect the same qualitative features for the case of an infinite conduction band.

ACKNOWLEDGMENTS

This work was supported by the National Science Foundation Grant No. DMR-86-17756, as well as by contributions from AT&T Bell Laboratories and Cray Research Corporation. Computations were performed on the Cray X-MP at the San Diego Supercomputer Center.

¹J. Friedel *Philos. Mag.* **43**, 153 (1952); *Can. J. Phys.* **34**, 1190 (1956); *Nuovo Cimento* **7**, 287 (1958).
²P. W. Anderson, *Phys. Rev.* **124**, 41 (1961).
³T. Moriya, *Progr. Theor. Phys.* **33**, 157 (1965); see also T. Moriya, in *Theory of Magnetism of Transition Metals, International School of Physics "Enrico Fermi", Course XXXVII*, edited by W. Marshall (Academic, New York, 1967).
⁴B. Coqblin and A. Blandin, *Adv. Phys.* **17**, 281 (1963).
⁵K. Yosida, A. Okiji, and S. Chikazumi, *Progr. Theor. Phys.* **33**, 559 (1965).

⁶J. R. Schrieffer, *J. Appl. Phys.* **38**, 1143 (1967).
⁷J. R. Schrieffer and P. A. Wolff, *Phys. Rev.* **149**, 491 (1966); see also, P. W. Anderson and A. M. Clogston, *Bull. Am. Phys. Soc.* **6**, 559 (1961); *J. Kondo. Prog. Theor. Phys.* **28**, 846 (1962).
⁸I. Okada and K. Yosida, *Progr. Theor. Phys.* **49**, 1483 (1973).
⁹B. Cornut and B. Coqblin, *Phys. Rev. B* **5**, 4541 (1972).
¹⁰Ph. Nozieres and A. Blandin, *J. Phys. (Paris)* **41**, 193 (1980).
¹¹K. Yamada, K. Yosida, and K. Hanzawa, *Progr. Theor. Phys.* **71**, 450 (1984).

- ¹²H. Shiba, *Progr. Theor. Phys.* **54**, 967 (1975).
- ¹³A. Yoshimori, *Progr. Theor. Phys.* **55**, 67 (1976).
- ¹⁴G. L. Lucas and D. C. Mattis, *Phys. Rev.* **178**, 854 (1969).
- ¹⁵A. M. Oles and K. A. Chao, *Phys. Stat. Sol. B* **103**, 769 (1981).
- ¹⁶J. E. Hirsch and R. M. Fye, *Phys. Rev. Lett.* **56**, 2521 (1986).
- ¹⁷J. R. Schrieffer and D. C. Mattis, *Phys. Rev.* **140**, 1412 (1965).
- ¹⁸K. Yamada, *Progr. Theor. Phys.* **53**, 1970 (1975); **54**, 316 (1975); K. Yosida and K. Yamada, *ibid.* **53**, 1286 (1975).
- ¹⁹J. E. Hirsch, *Phys. Rev. B* **28**, 4059 (1983).
- ²⁰P. Coleman and N. Andrei, *J. Phys. C* **19**, 3211 (1986); see also A. M. Tselick and P. B. Wiegmann, *Adv. Phys.* **32**, 453 (1983); and references therein.
- ²¹K. G. Wilson, *Rev. Mod. Phys.* **47**, 773 (1973); H. R. Krishna-Murthy, J. W. Wilkins, and K. G. Wilson, *Phys. Rev. B* **21**, 1003 (1981).
- ²²B. Caroli, C. Caroli, and D. R. Fredkin, *Phys. Rev.* **178**, 599 (1969).
- ²³L. Dworin and A. Narath, *Phys. Rev. Lett.* **25**, 1287 (1970).
- ²⁴P. H. Parmenter, *Phys. Rev. B* **8**, 1273 (1973).
- ²⁵J. E. Hirsch and H. Q. Lin, *Phys. Rev. B* **35**, 4943 (1987).
- ²⁶S. Alexander and P. W. Anderson, *Phys. Rev. A* **133**, 1594 (1964).
- ²⁷H. Q. Lin and J. E. Hirsch (unpublished).